

Calculation of the γ/γ' interface free energy in the Ni-Al system by the capillary fluctuation method

Y. Mishin*

School of Physics, Astronomy and Computational Sciences, MSN 3F3, George Mason University, Fairfax, Virginia 22030, USA

Abstract

Monte Carlo computer simulations with an embedded-atom potential are applied to study coherent γ/γ' interfaces in the Ni-Al system. The (100) interface free energy has been extracted from the power spectrum of equilibrium shape fluctuations (capillary waves) and found to decrease with temperature from about 20 mJ/m² at 550 K to about 10 mJ/m² at 1200 K. These numbers are in reasonable agreement with existing experimental data. Strengths and disadvantages of the capillary wave method are discussed.

Keywords: Interface free energy; capillary fluctuations; Monte Carlo simulation; Ni-Al system.

Interfaces between different phases control microstructural stability of many precipitation-hardened alloys. In particular, the coarsening kinetics of γ' -phase precipitates in the γ -phase matrix in Ni-based superalloys is largely controlled by the free energy σ of the γ/γ' interfaces [1]. Because reliable computational predictions of σ for multi-component commercial alloys are extremely difficult, attention has been focused on γ/γ' interfaces in the binary Ni-Al system as a model of superalloys. In the latter case, the γ -phase is an atomically disordered Ni-based solid solution whereas the γ' -phase is the intermetallic compound Ni₃Al (L1₂ structure) accommodating a few atomic per cent of off-stoichiometry. Even in this simpler case, however, calculations σ are challenging due to the complexity of the underlying interface thermodynamics [2, 3], issues with reliability of atomic interaction models, and the sheer volume of computations [2–5].

To further simplify the problem, several authors focused on coherent interfaces between pure Ni and perfectly stoichiometric Ni₃Al employing either first-principles calculations [6, 7] or atomistic simulations with empirical potentials [4, 8, 9]. In particular, Mao et al. [7] applied density functional theory calculations to compute σ as a function of temperature for three different low-index orientations of the interface. Their calculations include the ferromagnetic ordering, coherency strain energy and atomic vibrations. They predict that σ significantly decreases with temperature. For example, the (100) interface free energy

*Email: ymishin@gmu.edu

decreases from 27 mJ/m² at 0 K to about 23 mJ/m² at the temperature of 1000 K, demonstrating that the temperature effect should be taken into account for accurate calculations of σ .

An equally important factor that should also be taken into account is that at finite temperatures, the γ -phase is not pure Ni and the γ' -phase is not stoichiometric Ni₃Al. The actual chemical compositions of both phases and long-range order in the γ' -phase vary with temperature according to the Ni-Al phase diagram [10]. First-principles-based calculations of thermodynamic equilibrium between the γ and γ' phases could be pursued by the cluster expansion approach [11–13]. An alternate, and computationally more efficient, approach is offered by atomistic simulations with empirical potentials [4, 5]. For coherent γ/γ' interfaces, accurate but rather tedious calculations of σ could be performed by the thermodynamic integration method based on rigorous interface thermodynamic relations developed in [2, 3]. In this paper we explore a different route involving the analysis of capillary waves on the interfaces.

For rough interfaces supporting capillary waves, their equilibrium power spectrum can be analyzed to extract the interface free energy, or more accurately, the interface stiffness ($\sigma + \sigma''$), where σ'' is the second derivative of σ with respect to the interface inclination angle. For a narrow, ribbon-like interface geometry, the mean-squared amplitude (power) of capillary waves at a given temperature T is given by [14]

$$\langle a^2(k) \rangle = \frac{k_B T}{(\sigma + \sigma'') A k^2}, \quad (1)$$

where k_B is Boltzmann's factor, k is the wavenumber of the wave, and $A = wL$ is the interface area with L being the interface length and $w \ll L$ the interface ribbon width. Using the computed power spectrum, $(\sigma + \sigma'')$ can be determined from the slope of the plot $1/\langle a^2(k) \rangle$ versus k^2 . The capillary fluctuation method was applied to compute the free energies and stiffnesses of solid-liquid interfaces [14–22] and grain boundaries in single-component systems [23–25].

In this paper we apply this method to solid-solid phase boundaries in a binary system. This extension required solving the following problem. The previous applications of the method employed molecular dynamics simulations to measure the equilibrium fluctuation spectrum. Due to the well-known computational limitations, molecular dynamics simulations are usually run for times no longer than tens of nanoseconds. This time scale is too short to observe a significant amount of substitutional solute diffusion in the crystalline lattice even at high temperatures approaching the melting point. As a consequence, the computed capillary wave spectrum does not include fluctuation modes requiring diffusion-controlled redistribution of the solute between the crests and troughs of the waves. A possible answer would be to resort to lattice-free semi-grand canonical Monte Carlo simulations [26]. In this case, redistribution of the solute occurs by an artificially fast process involving random changes of the chemical species of the atoms. Although the dynamics of this process are unphysical, the simulation quickly and correctly samples numerous configurations representing the equilibrium state of the systems. This permits a fast calculation of the ensemble average value of $\langle a^2(k) \rangle$. In practice, however, it is impossible to adjust the chemical-potential difference $\Delta\mu$ between the species to *exactly* match the phase equilibrium condition. Consequently, the interface will always migrate towards one of the phases,

creating a dynamic situation that may affect the fluctuation spectrum. This unavoidable interface motion reflects the fact that the semi-grand canonical Monte Carlo method models an open system with neutral equilibrium between the phases. In this work this problem was addressed by imposing an additional constraint maintaining a fixed average composition of the two-phase system.

The simulation block had the approximate dimensions 28.6 by 50.0 by 1.4 nm with all-periodic boundary conditions and contained about 180,000 atoms. The z -dimension was relatively small to realize the ribbon-like geometry of the interface. The block initially contained two plane coherent (100) Ni/Ni₃Al interfaces normal to the y -axis. Atomic interactions were modeled by the embedded-atom potential developed in [4]. Monte Carlo simulations were run to equilibrate the system at a chosen temperature. The trial moves of the Monte Carlo process included (1) displacement of a randomly chosen atoms by a random amount in a random direction and (2) reassignment of its chemical species at random to either Ni or Al. The trial move was accepted or rejected according to the Metropolis algorithm, namely, with the probability $\exp(-\Phi/k_B T)$ if $\Phi > 0$ and unconditionally if $\Phi \leq 0$. Here

$$\Phi \equiv \Delta E \pm \Delta\mu \pm \frac{3}{2}k_B T \ln \frac{m_{\text{Ni}}}{m_{\text{Al}}}, \quad (2)$$

where m_{Ni} and m_{Al} are the atomic masses [27, 28]. The positive sign is used when Ni is replaced by Al and the negative when Al is replaced by Ni. The logarithmic term comes from integration of the probability distribution over the momenta of all atoms, producing a pre-exponential factor proportional to the product of all atomic masses to the power of 3/2. In the probability ratio of two configurations, all masses cancel out except for the atom whose species changes, producing a pre-exponential factor of either $(m_{\text{Ni}}/m_{\text{Al}})^{3/2}$ or $(m_{\text{Al}}/m_{\text{Ni}})^{3/2}$. Simultaneously with this Monte Carlo process, the zero-stress condition was maintained in each Cartesian direction by a Rahman-Parrinello algorithm.

To constrain the average fraction of Al atoms in the system, \bar{c} , to a preset target value \bar{c}_0 , a feedback loop was created between the current value of \bar{c} and the imposed chemical potential difference $\Delta\mu$. Namely, at each Monte Carlo step n , $\Delta\mu_n$ was modified by

$$\Delta\mu_n = \Delta\mu_{n-1} - \alpha \left(\frac{\bar{c}_{n-1} + \bar{c}_{n-2}}{2} - \bar{c}_0 \right), \quad (3)$$

where α is an adjustable constant. (One Monte Carlo step is defined as the number of trial moves equal to the number of atoms.) After a short transient, the system reached a regime in which its composition fluctuated around \bar{c}_0 accompanied by fluctuations of $\Delta\mu$ around a value $\Delta\mu_0$ corresponding to two-phase coexistence. At each temperature, \bar{c}_0 was chosen so that to create an equilibrium structure with nearly equal amounts of the phases. The described feedback loop is technically similar to the variance-constrained ensemble recently proposed by Sadigh et al. [29], although our implementation of Eq. (3) in the parallel Monte Carlo code was different.

Once phase equilibrium was reached, the Monte Carlo run was continued for approximately 10^6 steps to save a set of statistically independent snapshots and accurately compute average values of fluctuating parameters.

At the post-processing stage, every snapshot was quenched to 0 K to eliminate thermal noise. It was checked that the interfaces always remained perfectly coherent. For each atom

in a given snapshot, the local chemical composition ξ was computed as the fraction of Al atoms in a sphere of a radius 4 Å centered at the atom. The ξ numbers were then averaged over bulk regions unaffected by the interfaces to obtain the chemical compositions, c_γ and $c_{\gamma'}$, of the phases. To compute the interface shape, the x - y cross-section of the block was partitioned into imaginary cells (pixels) of equal size using a 300×400 mesh. The ξ numbers were averaged over each cell (including the z -direction) to obtain a coarse-grained chemical composition c assigned to each pixel (x_i, y_i) . In each row of pixels parallel to the y -direction (normal to the interface), c was a function of the pixel ordinate y_i . Namely, it remained nearly constant and equal to either c_γ or $c_{\gamma'}$ inside the phases and changed rapidly from one composition to the other in the interface regions. Using linear interpolation between neighboring pixels, for each interface the coordinate Y_i was found at which $c = (c_\gamma + c_{\gamma'})/2$ and was identified with the interface position at the given x_i . An example of interface profiles (x_i, Y_i) is shown in Fig. 1 where the points are connected by straight segments for clarity. The protrusions and zig-zags of the profile on the scale comparable to the unit cell size depend on the visualization parameters and do not represent in the physical shape of the interface. (The physical interface width could be evaluated from composition profiles *across* the interface averaged over the snapshots, which was not pursued in this work.) The discrete Fourier transformation was then applied to the discrete function $Y_i(x_i)$ and the Fourier amplitudes were averaged over a few hundred snapshots to obtain $\langle a^2(k_i) \rangle$ for a set of wavenumbers k_i . The phase compositions were also averaged over the same set of snapshots.

We assumed that the term σ'' could be neglected in comparison with σ . This cannot be proven rigorously but is consistent with the very rough shape of the interface studied here. The interface free energy was found by

$$\sigma = \frac{k_B T}{A \langle a^2(k) \rangle k^2}, \quad (4)$$

where the right-hand side is the slope of the plot $k_B T/A \langle a^2(k) \rangle$ versus k^2 .

Fig. 2 shows typical plots of $k_B T/A \langle a^2(k) \rangle$ versus k^2 and their mean-square linear fits. Significant deviations from linearity are observed at large k values when the amplitudes become comparable to the pixel size and cannot be resolved accurately. The linearity in the small k region confirms that Eq. (4) is a reasonable approximation.

The computed interface free energies were averaged over both interfaces present in the system and are summarized in Fig. 3. The plot starts at the temperature of 550 K because the amplitudes of the capillary waves decrease with temperature and could not be resolved below 550 K. On the high-temperature end, the simulations above 1200 K resulted in the rupture of the layers of the phases (Fig. 1) and formation of a single spherical γ' particle in the γ matrix. In the future, the temperature interval could be extended to higher temperatures by using wider layers of the phases to avoid their breakup.

Comparison of the calculated interface free energies with experiment is not straightforward for a number of reasons. The experimental values of σ are back-calculated from observations of coarsening kinetics of γ' particles. Such calculations rely on a kinetic model and a thermodynamic description of the alloy. Different σ values have been reported in the literature, depending on the choice of the kinetic and thermodynamic models. This can partially explain the significant scatter of the experimental data. For example, Fig. 3

includes earlier results [30] based on the Lifshitz-Slyozov-Wagner (LSW) [31, 32] model of coarsening together with more recent calculations [33] employing the trans-interface-diffusion-controlled (TIDC) model [34] with more accurate thermodynamics, both calculations utilizing the same set of experimental data. The plot also includes σ values for two ternary Ni-Al-Cr alloys obtained by applying the Kuehmann and Voorhees model [35] of coarsening to data measured by atom-probe tomography [36]. Another factor to consider is the possible anisotropy of σ suggested by previous calculations [4, 6, 7]. The experiments give σ averaged over all possible orientations. There is presently no experimental evidence of anisotropy of σ . Small γ' particles are spherical and transform to a cubic shape with (100) faces when they reach a certain size. However, this shape transformation is caused by misfit strains and the elastic anisotropy of the material and cannot be interpreted as evidence that $\sigma_{(100)}$ is smaller than for other crystallographic orientations (see discussion in [33]). On the other hand, the magnitude of σ is so small that it might still be anisotropic without affecting the particle shape. This possible anisotropy of σ also makes the comparison of the computed $\sigma_{(100)}$ values with average experimental values somewhat ambiguous.

Nevertheless, the computed σ values are approximately in the same ballpark as the known experimental data: 10 to 20 mJ/m². Although the agreement is imperfect, it is non-trivial given the extremely small magnitude of σ . Indeed, the computed σ is about 1-2% of the Al surface energy, below 1% of the Ni surface energy, and less than 1/3 of the surface tension of water at room temperature.

The main source of error in the reported σ is probably rooted in the inaccuracy of the atomistic potential [4]. As an illustration, Fig. 4 displays the computed γ and γ' solvus lines on the Ni-Al phase diagram. The phase compositions c_γ and $c_{\gamma'}$ at different temperatures were obtained as a side product in the calculations of the interface profiles. Both solvus lines agree with the previous calculation [4] by a different method using the same potential, but show significant deviations from the experimental phase diagram [37–39]. In particular, the compositional width of the ($\gamma + \gamma'$) field on the phase diagram is more narrow than in experiment, suggesting that the computed σ values are likely to be slightly underestimated. The accuracy of the calculations could be improved by developing a potential capable of reproducing the solvus lines in better agreement with experiment. Another factor neglected in this work is the effect of coherency strains. At several temperatures, the calculations were repeated by fixing the x -dimension of the simulation block at values creating slight lateral tensions or compressions on the level of $\pm 0.2\%$, modifying the coherency strains in the phases. No effect on σ was detected within the statistical errors of the calculations. However, if the accuracy of the method can be increased in the future, a way should also be found to take into account the coherency strains.

In conclusion, this work demonstrates that the capillary fluctuation method in conjunction with Monte Carlo simulations has a potential as a means of predicting free energies of γ/γ' interfaces and possibly other solid-solid interfaces with low free energies. The small magnitude of σ which makes it difficult to compute it by thermodynamic integration or similar methods leads to relatively large amplitudes of capillary waves and makes them amenable to spectral analysis allowing the extraction of σ . The values of σ computed in this work are in reasonable agreement with existing experimental data and show a significant decrease with temperature, approaching ~ 10 mJ/m² at high temperatures (Fig. 3).

I would like to thank A. J. Ardell, T. Frolov, A. Karma, D. N. Seidman and V. I. Ya-

makov for reading the manuscript and providing helpful comments. I am especially grateful to V. I. Yamakov for developing the parallel Monte Carlo code and making it available for this work. This research was sponsored by the National Institute of Standards and Technology, Material Measurement Laboratory, the Materials Science and Engineering Division.

References

- [1] C. T. SIMS, N. S. STOLOFF AND W. C. HAGEL, eds. *Superalloys II- High-Temperature Materials for Aerospace and Industrial Applications*. John Wiley and Sons/Wiley, New York, (1987).
- [2] T. FROLOV AND Y. MISHIN. Thermodynamics of coherent interfaces under mechanical stresses. I. Theory. *Phys. Rev. B* **85** (2012) 224106.
- [3] T. FROLOV AND Y. MISHIN. Thermodynamics of coherent interfaces under mechanical stresses. II. Application to atomistic simulation of grain boundaries. *Phys. Rev. B* **85** (2012) 224107.
- [4] Y. MISHIN. Atomistic modeling of the γ and γ' phases of the Ni-Al system. *Acta Mater.* **52** (2004) 1451–1467.
- [5] Y. MISHIN, M. ASTA AND J. LI. Atomistic modeling of interfaces and their impact on microstructure and properties. *Acta Mater.* **58** (2010) 1117 – 1151.
- [6] C. WANG AND C. Y. WANG. Ni/Ni₃Al interface: A density functional approach. *Appl. Surf. Sci.* **255** (2009) 3669–3675.
- [7] Z. MAO, C. BOOTH-MORRISON, E. PLOTNIKOV AND D. N. SEIDMAN. Effects of temperature and ferromagnetism on the γ -Ni/ γ' -Ni₃Al interfacial free energy from first principles calculations. *J. Mater. Sci.* **47** (2012) 7653–7659.
- [8] K. YASHIRO, M. NAITO AND Y. TOMITA. Molecular dynamics simulations of dislocation nucleation and motion at γ/γ' interface in Ni-based superalloy. *Int. J. Mech. Sci.* **44** (2002) 1845–1860.
- [9] T. ZHU AND C. Y. WANG. Misfit dislocation networks in the γ/γ' phase interface of a Ni-based single-crystal superalloy: Molecular dynamics simulations. *Phys. Rev. B* **72** (2005) 014111.
- [10] T. B. MASSALSKI, ed. *Binary Alloy Phase Diagrams*. ASM, Materials Park, OH, (1986).
- [11] M. SLUITER AND Y. KAWAZOE. A study of the thermodynamics of segregation and partial order at (111) antiphase boundaries in Ni₃Al. *Philos. Mag. A* **78** (1998) 1353–1364.
- [12] M. ASTA, V. OZOLIŅŠ AND C. WOODWARD. First principles approach to modeling alloy phase equilibria. *JOM* **53** (2001) 16–19.

- [13] A. VAN DE WALLE. Multicomponent multisublattice alloys, nonconfigurational entropy and other additions to the Alloy Theoretic Automated Toolkit. *Calphad Journal* **33** (2009) 266.
- [14] J. J. HOYT, M. ASTA AND A. KARMA. Method for computing the anisotropy of the solid-liquid interfacial free energy. *Phys. Rev. Lett.* **86** (2001) 5530–5533.
- [15] J. MORRIS. Complete mapping of the anisotropic free energy of the crystal-melt interface in Al. *Phys. Rev. B* **66** (2002) 144104.
- [16] J. MORRIS AND X. SONG. The anisotropic free energy of the Lennard-Johes crystal-melt interface. *J.Chem.Phys.* **119** (2003) 3920–3925.
- [17] J. J. HOYT, M. ASTA AND A. KARMA. Atomistic and continuum modeling of dendritic solidification. *Mater. Sci. Eng. R* **41** (2003) 121–163.
- [18] R. DAVIDCHACK, J. MORRIS AND B. LAIRD. The anisotropic hard-sphere crystal-melt interfacial free energy from fluctuations. *J. Chem. Phys.* **125** (2006) 094710.
- [19] C. A. BECKER, D. L. OLMSTED, M. ASTA, J. J. HOYT AND S. M. FOILES. Atomistic underpinnings for orientation selection in alloy dendritic growth. *Phys. Rev. Lett.* **98** (2007) 125701.
- [20] M. AMINI AND B. B. LAIRD. Crystal-melt interfacial free energy of binary hard spheres from capillary fluctuations. *Phys. Rev. B* **78** (2008) 144112.
- [21] C. A. BECKER, D. L. OLMSTED, M. ASTA, J. J. HOYT AND S. M. FOILES. Atomistic simulations of crystal-melt interfaces in a model binary alloy: Interfacial free energies, adsorption coefficients, and excess entropy. *Phys. Rev. B* **79** (2009) 054109.
- [22] R. E. ROZAS AND J. HORBACH. Capillary wave analysis of rough solid-liquid interfaces in nickel. *Europhys. Lett.* **93** (2011).
- [23] Z. T. TRAUTT AND M. UPMANYU. Direct two-dimensional calculations of grain boundary stiffness. *Scripta Mater.* **52** (2005) 1175–1179.
- [24] S. M. FOILES AND J. J. HOYT. Computation of grain boundary stiffness and mobility from boundary fluctuations. *Acta Mater.* **54** (2006) 3351–3357.
- [25] A. KARMA, Z. T. TRAUTT AND Y. MISHIN. Relationship between equilibrium fluctuations and shear-coupled motion of grain boundaries. *Phys. Rev. Lett.* **109** (2012) 095501.
- [26] D. FRENKEL AND B. SMIT. *Understanding molecular simulation: from algorithms to applications*. Academic, San Diego, second edition, (2002).
- [27] J. A. BROWN AND Y. MISHIN. Effect of Surface Stress on Ni Segregation in (110) NiAl Thin Films. *Phys. Rev. B* **69** (2004) 195407.

- [28] J. A. BROWN AND Y. MISHIN. Segregation and structural transformations at $\Sigma 3$ grain boundaries in NiAl: A Monte Carlo study. *Acta Mater.* **53** (2005) 2149–2156.
- [29] B. SADIGH, P. ERHAR, A. STUKOWSKI, A. CARO, E. MARTINEZ AND L. ZEPEDA-RUIZ. Scalable parallel Monte Carlo algorithm for atomistic simulations of precipitation in alloys. *Phys. Rev. B* **85** (2012) 184203.
- [30] A. J. ARDELL. Interfacial Free Energies and Solute Diffusivities from Data on Ostwald Ripening. *Interface Science* **3** (1995) 119–125.
- [31] I. M. LIFSHITZ AND V. V. SLYOZOV. The kinetics of precipitation from supersaturated solid solutions. *J. Phys. Chem. of Solids* **19** (1961) 35–50.
- [32] C. WAGNER. Theorie der Alterung von Niederschlägen durch Umlösen (Ostwald-Reifung). *Z. Elektrochem.* **65** (1961) 581–591.
- [33] A. J. ARDELL. Al-L₁₂ interfacial free energies from data on coarsening in five binary Ni alloys, informed by thermodynamic phase diagram assessments. *J. Mater. Sci.* **46** (2011) 4832–4849.
- [34] A. J. ARDELL AND V. OZOLIŅŠ. Trans-interface diffusion-controlled coarsening. *Nature Mater.* **4** (2005) 309–316.
- [35] C. J. KUEHMANN AND P. W. VOORHEES. Ostwald ripening in ternary alloys. *Metall. Mater. Trans. A* **27** (1996) 937–943.
- [36] C. BOOTH-MORRISON, J. WEININGER, C. K. SUDBRACK, Z. MAO, R. D. NOEBE AND D. N. SEIDMAN. Effects of solute concentrations on kinetic pathways in Ni–Al–Cr alloys. *Acta Mater.* **56** (2008) 3422–3438.
- [37] F. LI AND A. J. ARDELL. Coherent solubility limits of the γ' -type phases in Ni–Al, Ni–Ga and Ni–Ti alloys. *Scripta Mater.* **37** (1997) 1123–1128.
- [38] A. J. ARDELL. The Ni–Ni₃Al phase diagram: thermodynamic modeling and the requirements of coherent equilibrium. *Model. Simul. Mater. Sci. Eng.* **8** (2000) 277–286.
- [39] Y. MA AND A. J. ARDELL. The $(\gamma + \gamma')/\gamma'$ phase boundary in the Ni–Al phase diagram from 600 to 1200 C. *Z. Metallk.* **94** (2003) 972–975.

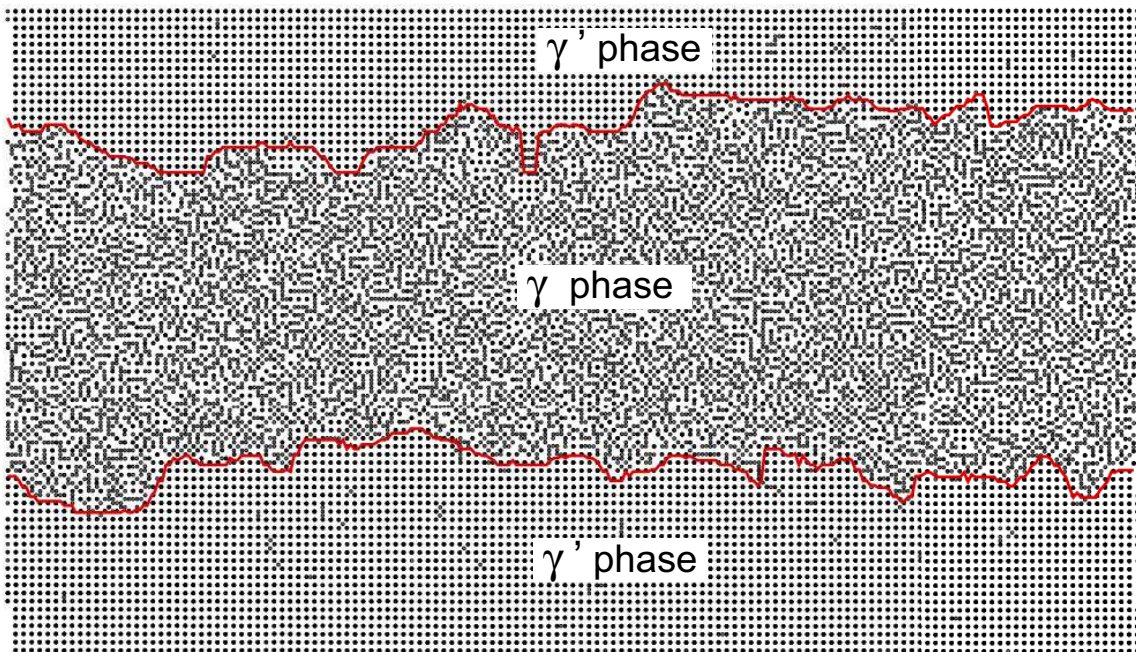


Figure 1: A typical snapshot of Monte Carlo simulations of γ and γ' phases at the temperature of 700 K. The simulation block is projected on the x - y plane showing only Al atoms. The red lines show the γ/γ' interfaces revealed by the visualization method applied in this work.

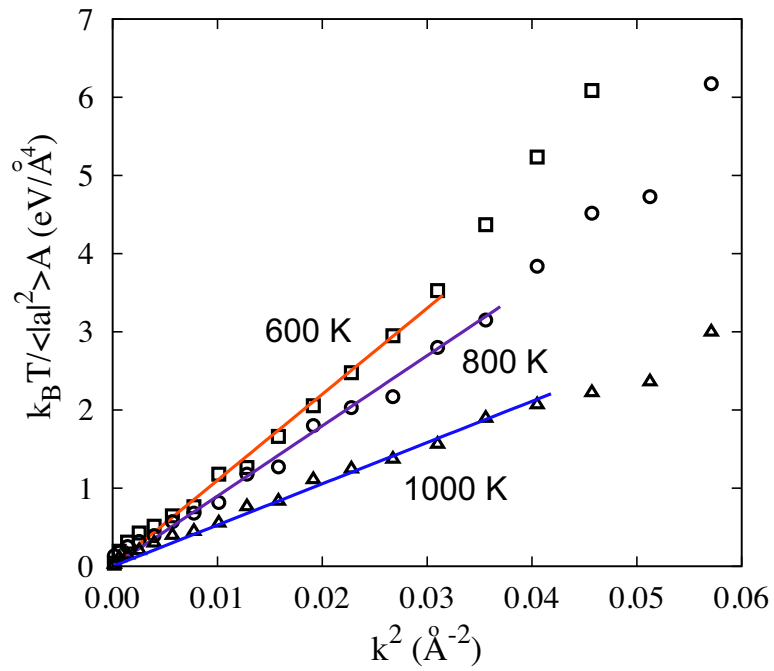


Figure 2: Typical plots of $k_B T / A \langle a^2(k) \rangle$ versus k^2 at three temperatures. The straight lines are linear fits in the long-wave range.

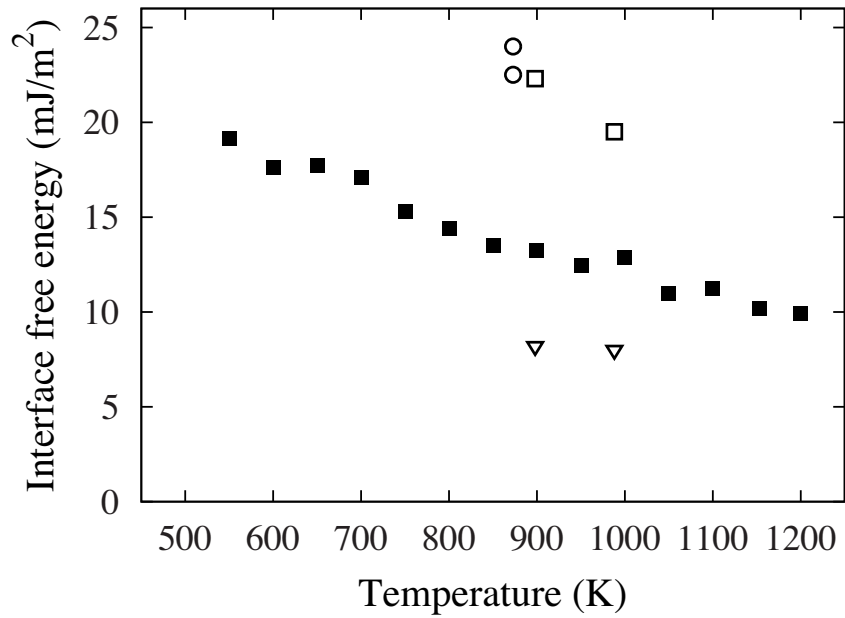


Figure 3: Comparison of (100) γ/γ' interface free energies σ computed by the capillary fluctuation method (filled squares) in comparison with experimental data for an average interface orientation: open triangles - Ni-Al system [30]; open squares - Ni-Al system with more accurate thermodynamics and TIDC model of coarsening [33]; open circles - Ni-Al-Cr alloys with different chemical compositions [36].

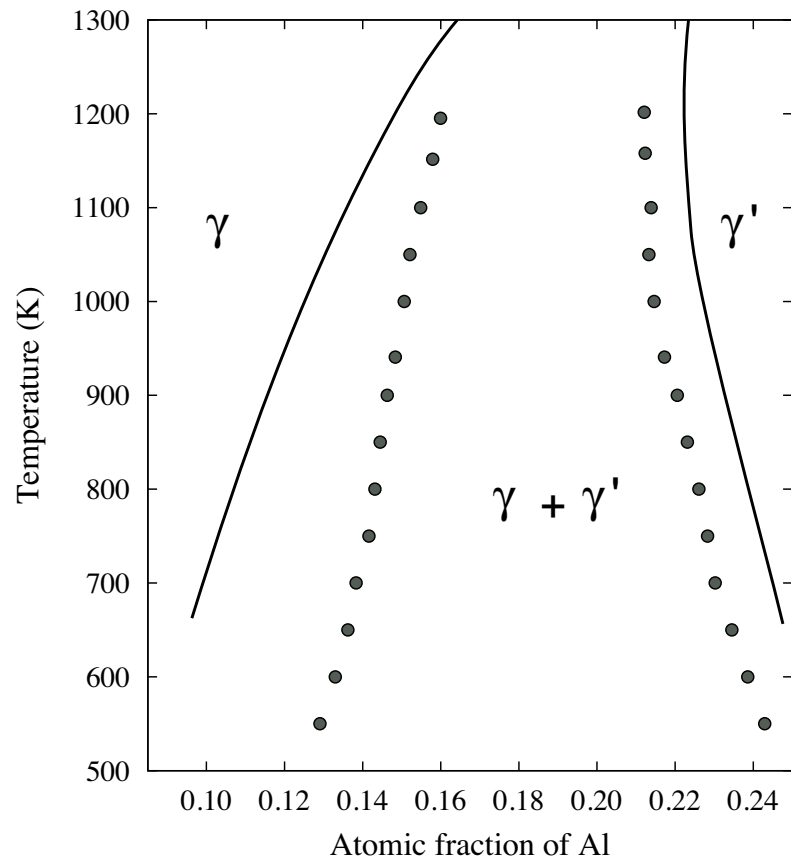


Figure 4: γ and γ' solvus lines on the Ni-Al phase diagram calculated in this work (points) in comparison with experiment [37–39] (lines).